

# Synthesis, Photo-physical and DFT Studies of ESIPT Inspired Novel 2-(2',4'-Dihydroxyphenyl) Benzimidazole, Benzoxazole and Benzothiazole

Vikas S. Patil · Vikas S. Padalkar · Abhinav B. Tathe ·  
Vinod D. Gupta · N. Sekar

Received: 17 January 2013 / Accepted: 30 April 2013 / Published online: 17 May 2013  
© Springer Science+Business Media New York 2013

**Abstract** Novel ESIPT inspired benzimidazole, benzoxazole and benzothiazole were synthesized from 2,4-dihydroxy benzoic acid and 1,2-phenylenediamine, 2-aminophenol, and 2-aminothiophenol respectively. The synthesized 2-(2',4'-dihydroxyphenyl) benzimidazole, benzoxazole and benzothiazole are fluorescent and the emission characteristic are very sensitive to the micro-environment. They show a single absorption and dual emission with large Stokes shift originating from excited state intramolecular proton transfer. The absorption-emission characteristics of all these compounds are studied as a function of pH. The change in the electronic transition, energy levels, and orbital diagrams of synthesized compounds were investigated by the molecular orbital calculation and were correlated with the experimental spectral emission. Experimental absorption and emission wavelengths are in good agreement with those predicted using the Density Functional Theory (DFT) and Time-Dependent Density Functional Theory (TD-DFT) [B3LYP/6-31G(d)].

**Keywords** ESIPT · Absorption-emission · pH sensitive · TD-DFT

## Introduction

There is a growing interest for environment sensitive materials due to potential applications in biotechnology such as biomedical and biosensing areas [1, 2]. Particularly the direct visualization of general biochemical events, specific molecular targets, or defined biochemical processes are indispensable for both in vitro [3–6] and, increasingly, in vivo applications [5–8]. These applications, because of the remarkable advances in imaging techniques, have begun to use an array of different fluorescent labels, probes, and sensors in multi-channel multiples studies [9–11] which include the real-time analysis of cells and whole organisms [12–15]. Dictated by the particular needs of several studies, fluorescent dyes and probes with defined optical, chemical, and biological properties are in high demand [16, 17]. Much effort has been focussed on the development of optical pH chemosensors [18–22] with specific attention paid to highly sensitive indicators within the physiological pH range [23, 24]. Two-band wavelength ratiometric sensing with a single dye is becoming increasingly important in this context [25] to measure pH by a two-band wavelength-ratiometric sensing both the acidic and basic states of the indicator should be ideally fluorescent and exhibit shifted absorption and dual-emission spectra. Obtaining two bands in emission spectra requires finding a dye with complex photo physics that exhibit an excited state reaction. In this case one of two bands belongs to the initially excited state and the other to the reaction product. If the molecule exhibits a fast (compared to the rate of fluorescence emission) and reversible excited state reaction, the two band ratiometric detection can provide self-calibration of fluorescence signal which allows compensation of all fluorescence quenching effects [26, 27].

The Excited State Intramolecular Proton Transfer (ESIPT) reactions generally incorporates transfer of a

V. S. Patil · V. S. Padalkar · A. B. Tathe · V. D. Gupta ·  
N. Sekar (✉)  
Tinctorial Chemistry Group, Institute of Chemical Technology  
(Formerly UDCT), N. P. Marg, Matunga,  
Mumbai 400 019, Maharashtra, India  
e-mail: n.sekar@ictmumbai.edu.in

V. S. Patil  
e-mail: vikasudct@gmail.com

V. S. Padalkar  
e-mail: vikaspadalkar@gmail.com

hydroxyl (or amino) proton to the carbonyl oxygen through a pre-existing hydrogen bonding configuration [28]. The resulting proton-transfer tautomer possesses significant differences in structure and electronic configuration from its corresponding normal species. The fundamental requirements of ESIPT process are the presence of intramolecular hydrogen bonding between the acidic proton, basic moiety and the suitable geometry of molecular system [29]. The acidic proton mostly used are  $-OH$ ,  $-NH_2$  etc. and basic centres are  $=N-$ , carbonyl oxygen ( $=C=O$ ). A large number of potential molecules [30] which show ESIPT are reported in literature and their absorption-emission properties are also studied as a function of their environment.

A variety of molecules have intramolecular hydrogen bonds (H-bonds) that may be photo induced to undergo proton transfer [31]. ESIPT can be observed in variety of such molecules that contain both hydrogen donor and acceptor in close proximity [32]. An intramolecular hydrogen bond generally formed in the ground state will migrate to the neighboring proton acceptor leading to a phototautomer [33]. In the general family of 2-(2'-hydroxyphenyl benzimidazole), benzoxazole, benzthiazole and benztriazole the ESIPT phototautomer gives rise to an emission with large stoke shift [34]. The high intensity of fluorescence emission and large stokes shift due to intramolecular proton transfer phenomena allow these molecules to have many interesting applications [35–37]. Molecules undergoing ESIPT exhibit dual fluorescence, one a normal stoke shifted fluorescence band which originates from a tautomer formed in the excited state (i.e. keto form) and second due to excited enol form. Further the fluorescence band maximum and the fluorescence quantum yield of the tautomer fluorescence band are very sensitive, whereas those of the normal band do not depend much on the environment. It is commonly understood that the molecular structure of the ESIPT compounds regulates their abnormal photo physical properties to a considerable extent, in most cases exceeding the influence of environment on them [34].

In this paper, we present the synthesis and characterization of new ESIPT unit hydroxyl benzimidazole, oxazole and thiazole. The absorption-emission characteristics of all these compounds were studied as a function of pH. The change in the electronic transition, energy levels, and orbital diagrams of synthesized compounds were investigated by the DFT computation and were correlated with the experimental photo-physical properties.

## Result and Discussion

### Chemistry

2-(2',4'-Dihydroxyphenyl)benzimidazole benzimidazole, benzoxazole and benzothiazole fluorescent derivatives **5–7**

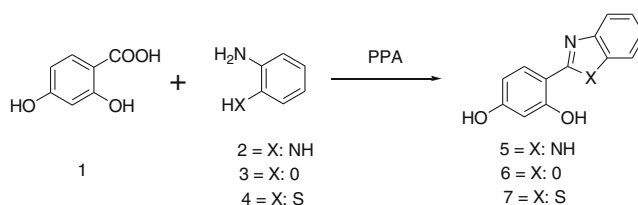
were prepared by the reaction of 2, 4-dihydroxy benzoic acid **1** with 1,2-phenylenediamines or *o*-aminophenol or *o*-aminothiophenol in the presences of polyphosphoric acid as shown in Scheme 1. All synthesised compounds were characterised by spectral analysis.

Synthesized benzimidazole, benzothiazole and benzoxazole molecules which contain acidic hydroxy group at 2'-position and 4'-position with respect to basic  $-N =$  moiety. The location of these groups is such that there is existence of intra-molecular hydrogen bonding in the ground state. On excitation, the  $-N =$  moiety become strongly basic and  $-OH$  group becomes strongly acidic. This leads to the ESIPT and thus the formation of keto isomer ( $k_1$ ).

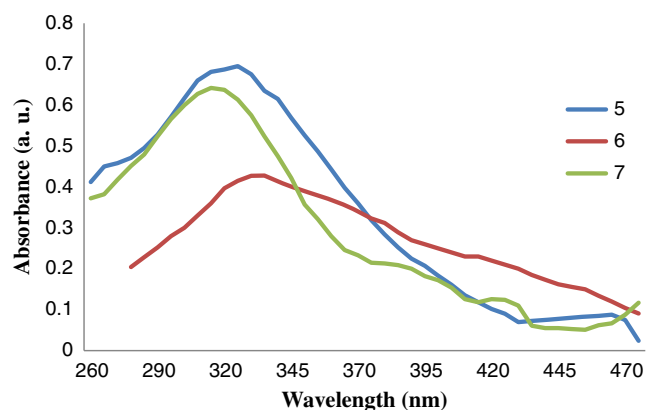
The ESIPT reactions of *o*-hydroxy and *o*-amino benzazoles (benzimidazole, benzoxazole and benzothiazole) have been studied extensively and it has been reported that *o*-amino benzazoles have lower fluorescent quantum yield accompanied by shorter Stokes shift as compared to the respective *o*-hydroxy benzazoles [38]. This observation has been explained in the light of the fact that  $NH_2$  group is low acidic compared to the  $-OH$  group. In addition improving the basicity of  $=N-$  on the azole ring will also help in accepting proton from the  $-OH$  or  $-NH_2$  facilitating the ESIPT phenomenon. In this paper we report ESIPT molecules where the basicity of  $=N-$  group on the azole ring is enhanced by the presence of  $-OH$  group on the phenyl ring at 2 and 4 position.

### Photophysical Properties

Synthesised compounds are highly fluorescent in solution under irradiation of UV light; absorption and emission of compounds were measured in water as well as in DMF. The absorption and fluorescence emission spectra of these compounds are shown in the Figs. 1, 2 and 3. All analyses were performed at room temperature and concentration was  $1 \times 10^{-6}$  M. The absorption and emission properties of compound in water and DMF are summarised in Table 1. The Stokes shift values of new compounds **5–7** are relatively higher than the reported hydroxy benzimidazole, benzoxazole and benzothiazole derivatives. The Stokes shift for molecules that do not show structural change in the excited state is generally found between 50 and 70 nm [37]. In contrast, novel compounds **5–7** exhibit ESIPT



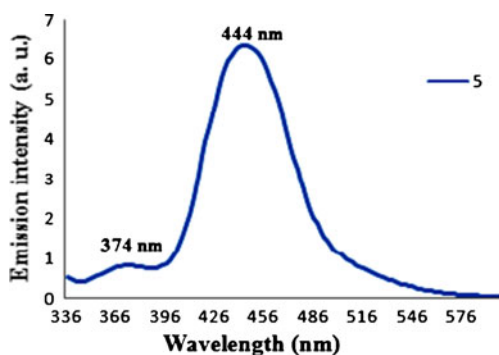
**Scheme 1** Synthesis of 4-(1H-benzo[d]imidazole, thiazole, oxazole-2-yl)benzene-1,3-diol



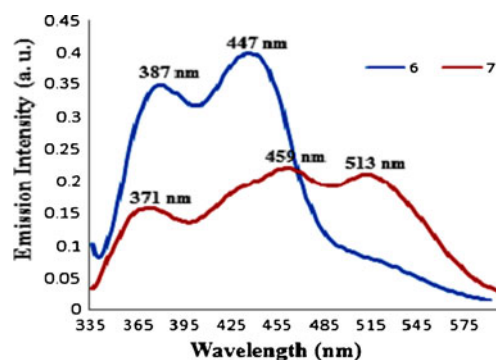
**Fig. 1** Absorption of compound 5, 6 and 7 in DMF

phenomena with Stokes shift between 42 and 148 nm. The occurrence of the dual emission of synthesised compound is clearly reflected in emission spectrum. The spectrum consists of two emission maxima ranging from 302 nm to 546 nm. Compounds 5–7 absorb in the range 317–335 nm and emit in the range 371–513 nm in DMF. Compounds 4–6 show multiple emissions due to ESIPT process. Compound 5 shorter emission (shoulder peak) observed at 374 nm and longer emission at 444 nm. In case of compound 6 shorter emission at 387 nm and longer emission at 447 nm. Compound 7 shows three emissions shortest at 371 nm, and longer emission at 513 nm in between these two emissions one more emission observed at 459 nm it may be due to rotamers of compounds. Quantum yields of compounds for short as well as longer emission were evaluated. Quantum yields of compounds 5–7 for short as well as long emission were evaluated and results are summarized in Table 1. Results reveal that Quantum yield is high at short emission as compared to longer emission.

Further we compared emission properties of synthesised compounds with its reported analogues 2(2'-hydroxyphenyl benzimidazole (2-HBI) [39], 2(2'-hydroxyphenyl benzoxazole (2-HBO) [40] and 2(2'-hydroxyphenyl benzothiazole (2-HBT) [41]. Emission properties of synthesised azoles 5–7 are same like reported 2-HBI, 2-



**Fig. 2** Emission spectra of compound 5 in DMF



**Fig. 3** Emission spectra of compound 6 and 7 in DMF

HBO and 2-HBT. The emission of 2-HBI (354 nm and 463 nm) are same like its 2,4-di hydroxy benzimidazole analogue 5 (374 and 444 nm). 2 (2'-Hydroxyphenyl benzoxazole shows single broad emission (506 nm), however 2 (2',4'-hydroxyphenyl benzoxazole 6 shows well splitted two emission shorter emission at 387 nm and longer emission at 447 nm. Blue shift is observed for 2(2',4'-dihydroxy benzimidazole. In case of thiazole analogue 2,4-dihydroxy substituted 7 shows three significant emission maxima shorter emission at 371 nm, longer emission at 513 nm and in between emission at 459 nm with high quantum yield (0.57), But 2-HBT shows dual emission, prominent peak at 510 nm and shoulder peak at 535 nm. Incorporation of hydroxy at 4-position with respect to azole ring enhances the ESIPT process in terms of well defined emission band.

#### Effect of pH

pH-Sensing is critical in chemistry and biology because it usually plays a pivotal role in a variety of systems. The most common pH sensors are glass electrodes. However, the known limitations of the glass pH electrodes make them unsuitable for certain applications like intracellular pH and microscopy studies. In contrast to the electrochemical methods, optical measurements based on fluorescent probes have no such limitations like common pH glass electrodes [42–46]. Moreover, fluorescent probes have their obvious advantages in terms of sensitivity, selectivity, and more convenient operations in many applications like remote sensing with optical fibers [46].

In the literature, various fluorescent compounds are reported as sensors for pH in the acidic region (less than 4). Rhodamine derivatives are extensively used as pH sensors because of their excellent photophysical properties like long absorption, emission wavelength, high quantum yield and good photostability. Fluorescent sensors for pH range 7–13 [46] are scarce. In this paper we report dual emitting fluorophores which show a large Stokes shift with good fluorescence intensity and quantum yield. Considering the

**Table 1** Absorption, emission and quantum yield of synthesized compounds 5–7 in DMF solvent

Compd	$\lambda_{\max}$ , nm	$\lambda_{\text{ems}}$ , nm (Short emission)	Stokes shift, $\text{cm}^{-1}$	Quantum yield at short emission	$\lambda_{\text{ems}}$ , nm (Long emission)	Stokes shift, $\text{cm}^{-1}$	Quantum yield at longer emission
5	326	374	3937	0.05	444	8152	0.11
6	335	387	4011	0.09	447	7479	0.13
7	317	371	4592	0.18	459 513	9759 12053	0.20 0.19

$\lambda_{\max}$  = absorption maxima;  $\lambda_{\text{ems}}$  = emission maxima;  $\epsilon$  = molar extinction coefficient

excellent properties of fluorophores we tested the effect of pH on fluorescence emission. Effect of pH on fluorescence emission was studied from pH 7–13 and results are summarised in Table 2. The results reveal that all the compounds are sensitive towards pH. All compounds show dual absorption at different pH with single emission, compounds emit approximately at the same wavelength at all pH. Absorption and emission spectra of compounds are shown in Figs. 4, 5 and 6.

#### Effect of Solvent Polarity

The investigation of solvent polarity on the absorption and fluorescence characteristics of organic compounds has been a subject of interest [47, 48]. Excitation of a molecule by photon causes a redistribution of charges leading to conformational changes in the excited state. The excited state is stabilized in solvents; the stability of excited state depends on polarities of solvent and dipole moment of compounds in excited state causes blue and red shift [47, 48]. Effects of solvent polarities on absorption and emission properties of compounds were studied in mixture of water and DMSO

ratio and results are summarised below, results reveals that all the compounds shows similar absorption and emission pattern in all the mixtures (Table 3).

#### Time Dependent Density Functional Theory

#### Structural Properties of Compounds 5–7

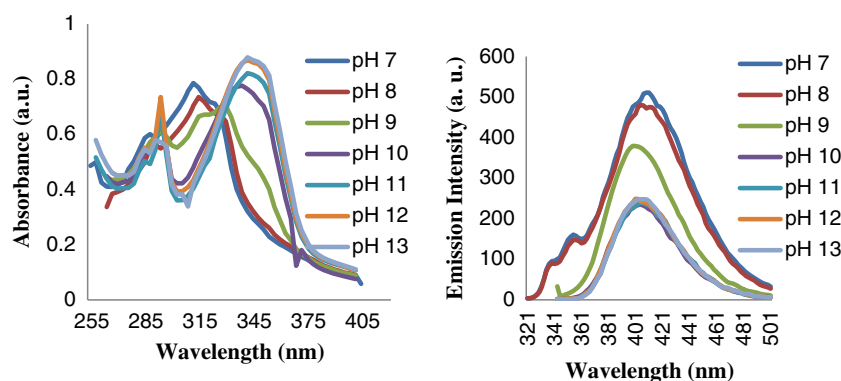
The structural changes due to ESIPT phenomenon in terms of bond angle, bond distances and geometry are investigated with the help of the optimized geometry at the B3LYP/6-31G(d) level of theory as shown in Table 4, 5 and 6. It clearly indicates that due to the intra-molecular hydrogen bonding the molecule has a six-member ring conformation in excited state. The molecular structures like stoichiometry, framework group, degree of freedom and point group of compounds remain the same in both the enol and keto forms Tables 4, 5 and 6 for all compounds. In compound 5 bond length [ $R_{\text{Enol}}(\text{O}_7\text{-C}_5)$ ; 1.341] and [ $R_{\text{Keto}}(\text{O}_7\text{-C}_5)$ ; 1.271] and bond angle [ $A_{\text{Enol}}(\text{N}_{13}\text{-C}_9\text{-N}_4)$ ; 128 and  $A_{\text{keto}}(\text{N}_{13}\text{-C}_9\text{-N}_4)$ ; 123] differ from each other in enol and keto form

**Table 2** Absorption and fluorescence spectra of compound 5–7 at various pH

pH	Compound 5		Compound 6		Compound 7	
	$\lambda_{\max}$ , nm ( $\epsilon$ , L. $\text{mol}^{-1}$ . $\text{cm}^{-1}$ )	$\lambda_{\text{ems}}$ , nm (intensity, a.u.)	$\lambda_{\max}$ , nm ( $\epsilon$ , L. $\text{mol}^{-1}$ . $\text{cm}^{-1}$ )	$\lambda_{\text{ems}}$ , nm (intensity, a.u.)	$\lambda_{\max}$ , nm ( $\epsilon$ , L. $\text{mol}^{-1}$ . $\text{cm}^{-1}$ )	$\lambda_{\text{ems}}$ , nm (intensity, a.u.)
7	315 (0.786)	410 (511)	291 (0.323) 336 (0.392)	450 (186)	294 (0.405) 345 (0.552)	404 (722)
8	291 (0.562) 315 (0.735)	410 (475)	291 (0.331) 330 (0.443)	450 (57)	291 (0.398) 315 (0.450)	416 (223)
9	294 (0.612) 330 (0.703)	398 (380)	291 (0.297) 333 (0.423)	448 (153)	291 (0.420) 330 (0.465)	408 (305)
10	294 (0.777) 339 (0.779)	404 (235)	294 (0.338) 336 (0.466)	448 (226)	291 (0.408) 330 (0.519)	406 (372)
11	294 (0.681) 342 (0.822)	404 (239)	294 (0.339) 375 (0.589)	443 (223)	294 (0.376) 351 (0.512)	400 (481)
12	294 (0.735) 342 (0.870)	400 (249)	294 (0.354) 375 (0.604)	450 (214)	294 (0.342) 351 (0.483)	400 (454)
13	294 (0.727) 342 (0.879)	406 (249)	294 (0.305) 375 (0.569)	450 (236)	294 (0.405) 345 (0.552)	404 (722)

$\lambda_{\max}$  = absorption maxima;  $\lambda_{\text{ems}}$  = emission maxima;  $\epsilon$  = molar extinction coefficient

**Fig. 4** Absorption and fluorescence spectra of compound **5** Vs pH



respectively, change in bond length clearly indicates ESIPT phenomenon observed in synthesised molecules. Similar trends observed for molecules **6** and **7**. Compounds **5–7** are roughly planar in enol and keto forms with dihedral angle is approximately  $0^\circ$  between two rings and facilitate excited state intra-molecular hydrogen transfer. In the enol form lone pair present on oxygen is involved in resonance. In this process single bond character is converted in to double bond character, bond length between O-H decreases as compared to keto form, this trend observed in all compounds. In ESIPT compounds change in bond length, bond angle and dihedral angle due to excited state intramolecular phenomenon for all compounds were summarised in Tables 4, 5 and 6. The bond length O-C of hydroxy is different for the enol and keto forms, the change in bond length clearly indicates that hydrogen is transferred in excited state and the enol form is (single bond, C-O) converted in keto form (double bond, C=O) by ESIPT. For the ESIPT process, the geometry between two rings is also very important.

#### *Vertical Excitation and Emission Study of Compounds 5–7 in Water and DMSO*

Compounds are fluorescent in solution on irradiation with UV light. Photophysical properties of compounds **5–7** were evaluated in water and DMSO solvents. Observed absorption and fluorescence properties were compared with absorption and emission obtained by DFT and TDDFT. Experimental observed absorption values of compounds are well in agreement with computed vertical excitation obtained by DFT. Compounds

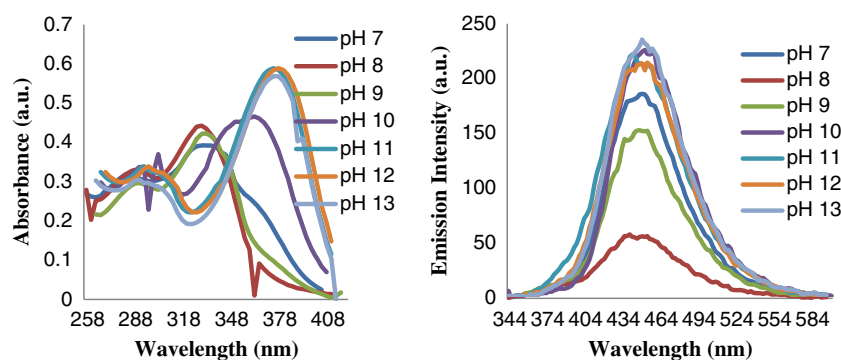
shows single emission in between 404–410 nm. Experimental emissions were compared with TDDFT emission. The difference between experimental mission and TD DFT emission is 40 nm. Compounds show dual emission in DMSO, short emission is well agreement with TDDFT emission. In water as well as in DMSO excitation is from HOMO-LUMO with almost same population. Observed absorption, emission, computed vertical excitations and emission are summarized in Table 7.

## Experimental

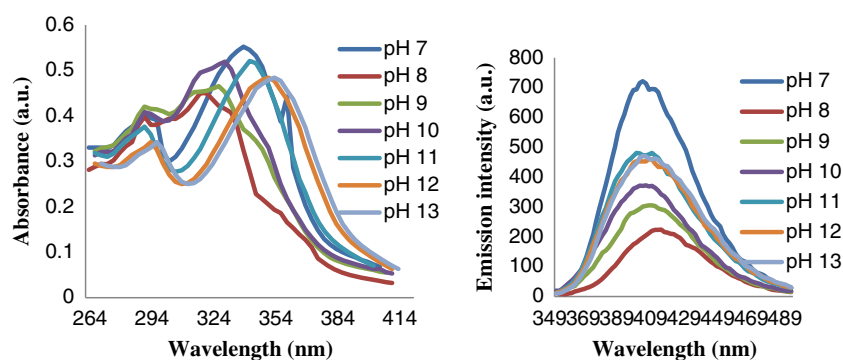
### General

All commercial reagents and solvents were procured from s. d. fine chemicals (India) and were used without purification. The reactions were monitored by TLC using on 0.25 mm E-Merck silica gel 60 F<sub>254</sub> precoated plates, which were visualized with UV light. Melting points were measured on standard melting point apparatus from Sunder industrial product Mumbai and are uncorrected. The FT- IR spectra were recorded on a Perkins-Elmer 257 spectrometer using KBr discs. <sup>1</sup>H NMR spectra were recorded on VXR 300-MHz instrument using TMS as an internal standard. LC-MS were recorded on FINNIGAN LCQ ADVANTAGE MAX instrument from Thermo Electron Corporation (USA). The absorption spectra of the compounds were recorded on a Spectronic Genesys 2 UV-Visible spectrophotometer; UV-Visible emission spectra were recorded on JASCO – FP 1520.

**Fig. 5** Absorption and fluorescence spectra of compound **6** Vs pH



**Fig. 6** Absorption and fluorescence spectra of compound **7** Vs pH



### Computational Methods

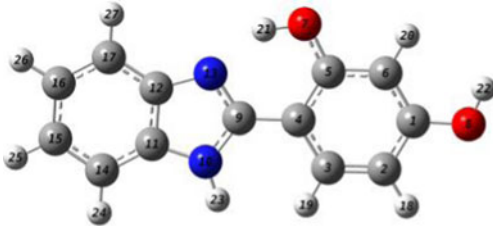
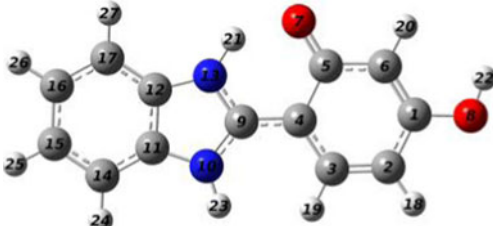
Compounds **5–7** were studied to find out electronic state and energy level by DFT computation methods. The ground state geometry of the compounds **5–7** in their  $C_s$  symmetry were optimized using the tight criteria in the gas phase using Density Functional Theory (DFT) [49]. The functional used was B3LYP. The B3LYP method combines Becke's three parameter exchange functional (B3) [50] with the nonlocal correlation functional by Lee, Yang and Parr (LYP) [51]. The basis set used for all atoms was 6-31G(d) [52–54]. The vibrational frequencies at the optimized structures were

computed using the same method to verify that the optimized structures correspond to local minima on the energy surface. The vertical excitation energies at the ground-state equilibrium geometries were calculated with TD-DFT [55]. The low-lying first singlet excited state ( $S_1$ ) of each tautomer was relaxed using the TD-DFT to obtain its minimum energy geometry. The difference between the energies of the optimized geometries at the first singlet excited state and the ground state was used in computing the emissions [56, 57]. All electronic structure computations were carried out using the Gaussian 09 program [58].

**Table 3** Effect of solvent polarity on absorption and emission properties of synthesized compounds

Compounds	Solvent ratio (Water/DMSO)	$\lambda_{\max}$ , nm	$\lambda_{\text{ems}}$ , nm	Stokes shift, $\text{cm}^{-1}$
5	20 % Water: 80% DMSO	319	358	3415
			446	8926
	40 % Water: 60% DMSO	319	355	3179
			440	8621
6	60 % Water: 40% DMSO	316	356	3556
			432	8497
	80 % Water: 20 % DMSO	316	356	3556
			420	7836
7	20 % Water: 80% DMSO	334	389	4233
			443	7367
	40 % Water: 60% DMSO	334	358	2007
			453	7865
7	60 % Water: 40% DMSO	334	389	4233
			447	7569
	80 % Water: 20 % DMSO	334	390	4299
			443	7367
7	20 % Water: 80% DMSO	322	358	3123
			411	6725
	40 % Water: 60% DMSO	319	363	3800
			428	7983
7	60 % Water: 40% DMSO	334	389	4233
			447	7569
	80 % Water: 20 % DMSO	319	355	3179
			416	7310


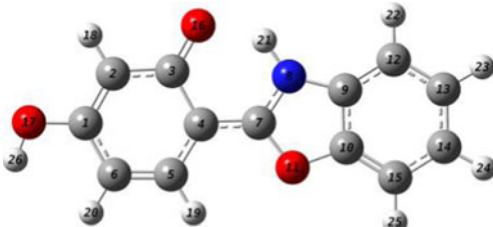
**Table 4** Structural properties of compound 5

Properties	5a (Enol)	5b (Keto)		
Stoichiometry	$C_{13}H_{10}N_2O_2$	$C_{13}H_{10}N_2O_2$		
Framework group	$C_1(\times(C_{13}H_{10}N_2O_2))$	$C_1(\times(C_{13}H_{10}N_2O_2))$		
Point group	$C_1$	$C_1$		
				
Bond distances	Bond	Bond length	Bond	Bond length
	R(O <sub>7</sub> -C <sub>5</sub> )	1.341	R(O <sub>7</sub> -C <sub>5</sub> )	1.271
	R(N <sub>13</sub> -C <sub>9</sub> )	1.328	R(N <sub>13</sub> -C <sub>9</sub> )	1.354
	R(C <sub>1</sub> -O <sub>8</sub> )	1.363	R(C <sub>1</sub> -C <sub>8</sub> )	1.364
Bond angle	Angle	Bond angle	Angle	Bond angle
	A(N <sub>13</sub> -C <sub>9</sub> -C <sub>4</sub> )	123	A(N <sub>13</sub> -C <sub>9</sub> -C <sub>4</sub> )	123
	A(O <sub>7</sub> -C <sub>5</sub> -C <sub>4</sub> )	122	A(O <sub>7</sub> -C <sub>5</sub> -C <sub>4</sub> )	122
Dihedral angle	A(N <sub>13</sub> -C <sub>9</sub> -C <sub>4</sub> -C <sub>5</sub> )	0.01	A(N <sub>13</sub> -C <sub>9</sub> -C <sub>4</sub> -C <sub>5</sub> )	0.00

Bond angle in degree,

Bond length in ° A Unit

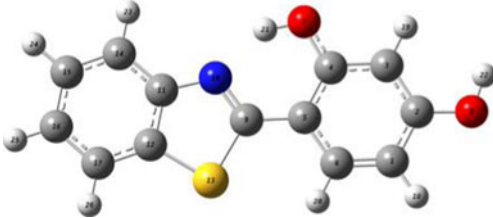
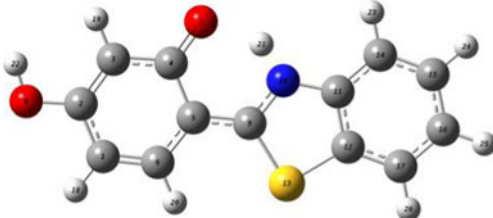
**Table 5** Structural properties of compound 6

Properties	6a (Enol)	6b (Keto)		
Stoichiometry	$C_{13}H_9NO_3$	$C_{13}H_9NO_3$		
Framework group	$C_1(\times(C_{13}H_9NO_3))$	$C_1(\times(C_{13}H_9NO_3))$		
Point group	$C_1$	$C_1$		
				
Bond distances	Bond	Bond length	Bond	Bond length
	R(O <sub>16</sub> -C <sub>3</sub> )	1.343	R(O <sub>16</sub> -C <sub>3</sub> )	1.270
	R(N <sub>8</sub> -C <sub>7</sub> )	1.311	R(N <sub>8</sub> -C <sub>7</sub> )	1.345
	R(C <sub>1</sub> -O <sub>17</sub> )	1.362	R(C <sub>1</sub> -O <sub>17</sub> )	1.364
Bond angle	Angle	Bond angle	Angle	Bond angle
	A(N <sub>8</sub> -C <sub>7</sub> -C <sub>4</sub> )	126	A(N <sub>8</sub> -C <sub>7</sub> -C <sub>4</sub> )	124
	A(C <sub>4</sub> -C <sub>3</sub> -O <sub>16</sub> )	122	A(C <sub>4</sub> -C <sub>3</sub> -O <sub>16</sub> )	122
Dihedral angle	A(N <sub>8</sub> -C <sub>7</sub> -C <sub>4</sub> -C <sub>3</sub> )	0.00	A(N <sub>8</sub> -C <sub>7</sub> -C <sub>4</sub> -C <sub>3</sub> )	0.01

Bond angle in degree,

Bond length in ° A Unit

**Table 6** Structural properties of compound 7

Properties	7a (Enol)	7b (Keto)		
Stoichiometry	C <sub>13</sub> H <sub>9</sub> NSO <sub>2</sub>	C <sub>13</sub> H <sub>9</sub> NSO <sub>2</sub>		
Framework group	C <sub>1</sub> (×(C <sub>13</sub> H <sub>9</sub> NSO <sub>2</sub> ))	C <sub>1</sub> (×(C <sub>13</sub> H <sub>9</sub> NSO <sub>2</sub> ))		
Point group	C <sub>1</sub>	C <sub>1</sub>		
				
Bond distances	Bond	Bond length	Bond	Bond length
	R(N <sub>10</sub> -C <sub>9</sub> )	1.311	R(N <sub>10</sub> -C <sub>9</sub> )	1.347
	R(O <sub>7</sub> -C <sub>4</sub> )	1.341	R(O <sub>7</sub> -C <sub>4</sub> )	1.270
	R(C <sub>2</sub> -O <sub>8</sub> )	1.361	R(C <sub>2</sub> -O <sub>8</sub> )	1.361
Bond angle	Angle	Bond angle	Angle	Bond angle
	A(N <sub>10</sub> -C <sub>9</sub> -C <sub>5</sub> )	123	A(N <sub>10</sub> -C <sub>9</sub> -C <sub>5</sub> )	122
	A(C <sub>4</sub> -C <sub>5</sub> -C <sub>9</sub> )	119	A(C <sub>4</sub> -C <sub>5</sub> -C <sub>9</sub> )	117
	A(O <sub>7</sub> -C <sub>4</sub> -C <sub>5</sub> )	122	A(O <sub>7</sub> -C <sub>4</sub> -C <sub>5</sub> )	122
Dihedral Angle	A(N <sub>10</sub> -C <sub>9</sub> -C <sub>5</sub> -C <sub>4</sub> )	0.00	A(N <sub>10</sub> -C <sub>9</sub> -C <sub>5</sub> -C <sub>4</sub> )	0.00

Bond angle in degree,

Bond length in °A Unit

## Relative Quantum Yield Calculations

Quantum yield of synthesized compounds in different solvents were calculated by using anthracene as reference standard in different solvents using the comparative method

[59–63]. Absorption and emission characteristics of the standard and the compounds in polar as well as non-polar solvents were measured at different concentrations at (2, 4, 6, 8, and 10 ppm level). Emission intensity values were plotted against absorbance values and linear plots were

**Table 7** Observed UV-visible absorption, emission and computed vertical excitation and emission of compounds 5–7 in water and DMSO

Compd	Experimental absorption, λ <sub>max</sub> , nm	Vertical excitation (TDDFT)		<i>f</i>	% Deviation	Assignment	Observed emission, λ <sub>ems</sub> , nm	Stokes shift, cm <sup>-1</sup>	TD-DFT emission, λ <sub>ems</sub> , nm
		nm	eV						
5 <sup>a</sup>	315	307	4.0257	0.63	2.5	H→L (0.6325)	410	7356	367
6 <sup>a</sup>	336	321	3.9801	0.73	4.4	H→L (0.7019)	450	7540	375
7 <sup>a</sup>	294	333	3.7207	0.75	13	H→L (0.6463)	404	9261	357
5 <sup>b</sup>	311	311	3.9741	0.81	0.0	H→L (0.6530)	360 <sup>c</sup> 446 <sup>d</sup>	4377 9733	367
6 <sup>b</sup>	334	315	3.9305	0.88	5.6	H→L (0.6469)	366 <sup>c</sup> 446 <sup>d</sup>	2618 7519	375
7 <sup>b</sup>	322	335	3.6941	0.80	4.0	H→L (0.6502)	381 <sup>c</sup> 384 <sup>d</sup>	4809 5014	394

<sup>a</sup> Absorption and emission were measured in Water solvent<sup>b</sup> Absorption and emission were measured in DMSO solvent<sup>c</sup> Observed emission at shorter wavelength<sup>d</sup> Observed emission at longer wavelength*f*: Oscillator Strength



obtained. Gradients were calculated for compounds in each solvent and for the standards. All the measurements were done by keeping the parameters constant such as solvent and slit width. Relative quantum yields of synthesized compounds in different solvents were calculated by using Eq. 1 [59–63].

$$\phi_x = \Phi_{st} \times \frac{Grad_x}{Grad_{st}} \times \frac{\eta_x^2}{\eta_{st}^2} \quad (1)$$

Where:

$\Phi_x$	Quantum yield of compound
$\Phi_{st}$	Quantum yield of standard sample
$Grad_x$	Gradient of compound
$Grad_{st}$	Gradient of standard sample
$\eta_x$	Refractive index of solvent used for synthesized compound
$\eta_{st}$	Refractive index of solvent used for standard sample

#### Synthesis of Compounds 5–7

##### *Synthesis of 4-(1H-benzo[d]imidazol-2-yl)benzene-1,3-diol (5)*

2,4-Dihydroxy benzoic acid **1** (10 g, 64.9 mmol), and *o*-phenylenediamine **2** (7.01 g, 64.9 mmol) were mixed in polyphosphoric acid (121.94 g). The mixture was stirred at 250 °C for 4 h and then it was allowed to cool at room temperature, poured into 1,200 mL ice-cold water with constant stirring. Dark brown precipitate was obtained which was filtered and dissolved in cold solution of 10 % Na<sub>2</sub>CO<sub>3</sub> (15.75 g dissolved in 137 mL of water) acidified with 1:1 HCl (40 mL) at 10 °C. This solution was kept overnight at 0 °C to give the final product **5**. Compound was recrystallized from ethanol.

Yield 54 %, Melting point = >300 °C.

**<sup>1</sup>H NMR (CD<sub>3</sub>)<sub>2</sub>SO**:  $\delta$  6.88 (d, 1H,  $J=6.4$  Hz), 6.88 (d, 1H,  $J=6.4$  Hz), 7.05 (s, 1H), 7.34 (s, 2H), 7.71 (s, 2H), 8.07 (s, 1H), 11.2 (s, 1H) ppm.

**FT-IR (KBr)**: 3438 (phenolic O-H), 3322 (N-H), 1651 (imine C = N), 1571 (aromatic C = C), 1516, 1421, 1389, 1203 (phenol C-O) cm<sup>-1</sup>.

**Mass**:  $m/z$  226 (M<sup>+</sup>).

##### *Synthesis of (1H-benzo[d]thiazole-2-yl)benzene-1,3-diol (6)*

2,4-Dihydroxy benzoic acid **1** (10 g, 64.9 mmol), and *o*-aminothiophenol **3** (8.11 g, 64.9 mmol) were mixed in polyphosphoric acid (121.94 g). The mixture was stirred at 150 °C for 4 h and then it was allowed to cool to room temperature, poured into 1,200 mL ice-cold water with constant stirring. Dark green precipitate was obtained. It was filtered and dissolved in cold solution of 10 % Na<sub>2</sub>CO<sub>3</sub> (15.75 g dissolved in

137 mL of water) acidified with 1:1 HCl (40 mL) at 10 °C. This solution was kept overnight at 0 °C to give the product **6**. Compound was recrystallized from ethanol.

Yield: 61 %, Melting point = >300 °C.

**<sup>1</sup>H-NMR (CD<sub>3</sub>)<sub>2</sub>SO**:  $\delta$  6.25 (m, 2H), 6.82 (d, 1H  $J=8.9$  Hz), 6.95 (d, 1H  $J=9.1$  Hz), 7.59 (d, H), 7.82 (m, 2H). 10.60 (s, 2H) ppm.

**FT-IR (KBr<sup>1</sup>)**: 3341 (phenolic O-H stretching), 1696 (amide C = O), 1651 (imine C = N), 1583 (aromatic C = C), 1501, 1448, 1422, 1215 (phenol C-O) cm<sup>-1</sup>.

**MASS**:  $m/z$ : 243 (M<sup>+</sup>).

##### *Synthesis of (1H-benzo[d]oxazole-2-yl)benzene-1,3-diol (7)*

2,4-Dihydroxy benzoic acid **1** (10 g, 64.9 mmol), and *o*-aminophenol **4** (7.07 g, 64.9 mmol) were mixed in polyphosphoric acid (121.94 g). The mixture was stirred at 150 °C for 4 h and then it was allowed to cool to room temperature, poured into 1,200 mL ice-cold water with constant stirring. Dark green precipitate was obtained. It was filtered and dissolved in cold solution of 10 % Na<sub>2</sub>CO<sub>3</sub> (15.75 g dissolved in 137 mL of water) acidified with 1:1 HCl (40 mL) at 10 °C. This solution was kept overnight at 0 °C to give the product **7**. Compound was recrystallized from ethanol.

Yield: 63 %, Melting point = >300 °C.

**<sup>1</sup>H-NMR (CD<sub>3</sub>)<sub>2</sub>SO**:  $\delta$  6.87 (s, 1H), 6.9 (s, 2H), 7.56 (d, H,  $J=7.3$  Hz), 7.89 (d, H,  $J=7.3$  Hz), 8.2 (s, 2H), 11.71(s, 1H) ppm.

**FT-IR (KBr)**: 3315 (phenolic O-H stretching), 1679 (amide C = O), 1647 (imine C = N), 1611 (aromatic C = C), 1567, 1237 (phenol C-O) cm<sup>-1</sup>.

**MASS**:  $m/z$ : 227 (M<sup>+</sup>).

#### Conclusion

Novel dual emitting 2-substituted benzimidazole, benzothiazole and benzoxazole were synthesised. The photophysical properties, absorption and emission of the compounds **5–7** in DMF were obtained experimentally and correlated with the computational results. Computed absorption and emission of the compounds are in good agreement with the experimental results. Structural properties of the compounds were evaluated for the keto as well as enol form, and the results clearly indicate that the ESIPT process is observed in the present compounds. The effect of pH and polarity of solvents on the photophysical properties were studied at pH range 7–13 and the results reveal that the compounds are sensitive towards pH and solvent polarity.

**Acknowledgments** Vikas Patil and Vikas Padalkar are thankful to the Institute of Chemical Technology, Mumbai, India.

## References

1. Malhotra BD, Turner APF (2003) *Advances in biosensors 4: perspectives in biosensors*. Elsevier, UK
2. Damia B, Peter DH (2010) *Biosensors for the environmental monitoring of aquatic systems*. Springer-Verlag Berlin and Heidelberg GmbH & Co. KG, Berlin
3. Johnsson N (2007) Chemical tools for biomolecular imaging. *ACS Chem Biol* 2:31–38
4. Unciti-Broceta A, Díaz-Mochón J, Mizomoto H, Bradley M (2008) pH sensing in living cells using fluorescent microspheres. *J Comb Chem* 10:179–184
5. Domaille D, Que E, Chang C (2008) Synthetic fluorescent sensors for studying the cell biology of metals. *J Nat Chem Biol* 4:168–175
6. Giepmans B, Adams S, Ellisman M, Tsien R (2006) The fluorescent toolbox for assessing protein location and function. *Science* 312:217–224
7. Weissleder R, Ntziachristos V (2003) Shedding light onto live molecular targets. *Nat Med* 9:123–128
8. Zhang J, Campbell R, Ting A, Tsien R (2002) Creating new fluorescent probes for cell biology. *Nat Rev Mol Cell Biol* 3:906–918
9. Díaz-Mochón J, Tourniaire G, Bradley M (2007) Microarray platforms for enzymatic and cell-based assays. *Chem Soc Rev* 36:449–457
10. Pernagallo S, Unciti-Broceta A, Díaz-Mochón J, Bradley M (2008) Deciphering cellular morphology and biocompatibility using polymer microarrays. *Biomed Mater* 3:34112–34118
11. Unciti-Broceta A, Diezmann F, Ou-Yang C, Fara M, Bradley M (2009) Synthesis penetrability and intracellular targeting of fluorescein-tagged peptides and peptide-peptoid hybrids. *Bioorg Med Chem* 17:959–966
12. Lavis L, Raines R (2008) Bright ideas for chemical biology. *ACS Chem Biol* 3:142–155
13. Hell S (2003) Toward fluorescence nanoscopy. *Nat Biotechnol* 11:1347–1355
14. Weissleder R (2006) Molecular imaging in cancer. *Science* 312:1168–1171
15. Alexander L, Dhaliwal K, Simpson J, Bradley M (2008) Dunking doughnuts into cells—selective cellular translocation and in vivo analysis of polymeric micro-doughnuts. *Chem Commun* 30:3507–3509
16. Thommes PT, Mon TM, Jing YY, Kimberly C, Alina K, James B, Peter C, Theodore BN, James RB (2004) Detection and analysis of tumor fluorescence using a Two-photon optical fiber probe. *Biophysics J* 86(6):3959–3965
17. Bingshuai W, Fabiao Y, Peng L, Xiaofei S, Keli H (2013) A BODIPY fluorescence probe modulated by selenoxide spirocyclization reaction for peroxynitrite detection and imaging in living cells. *Dyes Pigment* 96:383–390
18. Charier S, Ruel O, Baudin JB, Alcor D, Allemand JF, Meglio A, Jullien L (2004) An efficient fluorescent probe for ratiometric pH measurements in aqueous solutions. *Angew Chem Int Ed* 43:4785–4788
19. Wong LS, Birembaut F, Bocklesby WS, Frey JG, Bradley M (2005) Resin bead micro-UV-Visible absorption spectroscopy. *Anal Chem* 77:2247–2251
20. Cho JK, Wong LS, Dean TW, Ichihara O, Muller C, Bradley M (2004) pH indicating resins. *Chem Commun* 13:1470–1471
21. Cho JK, White PD, Klute W, Dean TW, Bradley M (2003) Self-indicating resins: sensor beads and in situ reaction monitoring. *J Comb Chem* 5:632–636
22. Wong LS, Brocklesby WS, Bradley M (2005) Fibre optic pH sensors employing tethered non-fluorescent indicators on macroporous glass. *Sens Actuator B Chem* 107:957–962
23. Bradley M, Alexander L, Duncan K, Chennaoui M, Jones AC, Sanchez-Martin RM (2008) pH sensing in living cells using fluorescent microspheres. *Bioorg Med Chem Lett* 18:313–317
24. Vasylevska AS, Karasyov AA, Borisov SM, Krause C (2007) Fluorescent pH indicators, probes and membranes covering a broad pH range. *Anal Bioanal Chem* 387:2131–2141
25. Demchenko AP (2009) *Introduction to fluorescence sensing*, Springer Science + Business Media B.V.
26. Demchenko AP (2005) The problem of self-calibration of fluorescence signal in microscale sensor systems. *Lab Chip* 5:1210–1223
27. Demchenko AP (2005) The future of fluorescence sensor arrays. *Trends Biotechnol* 23:456–460
28. Basaric N, Wan P (2006) Competing excited state intramolecular proton transfer pathways from phenol to anthracene moieties. *J Org Chem* 71:2677–2686
29. Sinha H, Dogra S (1986) Ground and excited state prototropic reactions in 2-(*o*-hydroxyphenyl) benzimidazole. *Chem Phys* 102:337–347
30. Douhal A, Amat-Guerri F, Lillo M, Acuna A (1994) Proton transfer spectroscopy of 2-(2'-hydroxyphenyl) imidazole and 2-(2'-hydroxyphenyl) benzimidazole dyes. *J Photochem Photobiol A Chem* 78:127–138
31. Min WC, Tsung YL, Cheng CH, Kuo CT, Hungshin F, Pi TC, Shen HY, Yun C (2010) Excited-state intramolecular proton transfer (ESIPT) fine tuned by quinoline-pyrazole isomerism:  $\pi$ -conjugation effect on ESIPT. *J Phys Chem A* 114:7886–7891
32. Douhal A, Amat GF, Acuna AU (1997) Probing nanocavities with proton-transfer fluorescence. *Angew Chem Int Ed Engl* 36:1514–1516
33. Huang J, Peng AD, Fu HB, Ma Y, Zhai TY, Yao JN (2006) Temperature-dependent ratiometric fluorescence from an organic aggregates system. *J Phys Chem A* 110:9079–9083
34. Padalkar VS, Tathe AB, Gupta VD, Patil VS, Phatangare KR, Sekar N (2012) Synthesis and photo-physical characteristics of ESIPT inspired 2-substituted benzimidazole, benzoxazole and benzothiazole fluorescent derivatives. *J Fluoresc* 22:311–322
35. Minkin VI, Garnovskii AD, Elguero J, Katritzky AR, Denisko OV (2000) The tautomerism of heterocycles: five-membered rings with two or more heteroatoms. *Adv Heterocyc Chem* 76:157–323
36. Doroshenko A, Posokhov E, Verezubova A, Ptyagina L (2000) Excited state intramolecular proton transfer reaction and luminescent properties of the ortho-hydroxy derivatives of 2,5-diphenyl-1,3,4-oxadiazole. *J Phys Org Chem* 13:253–265
37. Zhao J, Ji S, Chen Y, Guo H, Yang P (2012) Excited state intramolecular proton transfer (ESIPT): from principal photophysics to the development of new chromophores and applications in fluorescent molecular probes and luminescent materials. *Phys Chem Chem Phys* 14:8803–8817
38. Sandra S, Dogra S (1999) Excited state intramolecular protons transfer in 2-(2'-*N*-palmitoyl-aminophenyl) benzimidazole: effect of carbonyl group. *J Mol Struct* 476:223–233
39. Douhal A, Amat GF, Lillo M, Acuna A (1994) Proton transfer spectroscopy of 2-(2'-hydroxyphenyl)imidazole and 2-(2'-hydroxyphenyl)benzimidazole dyes. *J Photochem Photobiol A Chem* 78:127–138
40. Williams D, Heller A (1970) Intramolecular proton transfer reactions in excited fluorescent compounds. *J Phys Chem* 74:4473–4480
41. Anthony K, Brown R, Hepworth J, Hodgson K, May B (1984) Solid-state fluorescent photophysics of some 2-substituted benzothiazoles. *J Chem Soc Perkin Trans* 2:2111–2117
42. Tian M, Peng X, Fan J, Wang J, Sun S (2012) A fluorescent sensor for pH based on rhodamine fluorophore. *Dyes Pigments* 95:112–115

43. Ogikubo S, Nakabayashi T, Adachi T, Islam MS, Yoshizawa T, Kinjo M (2011) Intracellular pH sensing using autofluorescence lifetime microscopy. *J Phys Chem B* 115(34):10385–10390
44. Zhang WS, Tang B, Liu X, Liu YY, Xu KH, Ma JP (2009) A highly sensitive acidic pH fluorescent probe and its application to HepG2 cells. *Analyst* 134(2):367–371
45. Kim HN, Guo ZQ, Zhu WH, Yoon J, Tian H (2011) Recent progress on polymer-based fluorescent and colorimetric chemosensors. *Chem Soc Rev* 40(1):79–93
46. Han J, Burgess K (2010) Fluorescent indicators for intracellular pH. *Chem Rev* 110:2709–2728
47. Patil NR, Melavanki RM, Kapatkar SB, Ayachit NH, Saravanan J (2011) *J Fluoresc* 21:1213–1222
48. Melavanki RM, Patil NR, Kapatkar SB, Ayachit NH, Umapathy S, Thipperudrappa J, Nataraju AR (2011) *J Mol Liq* 158(2):105–110
49. Treutler O, Ahlrichs R (1995) Efficient molecular numerical integration schemes. *J Chem Phys* 102:346–354
50. Becke AD (1993) A new mixing of Hartree-Fock and local density-functional theories. *J Chem Phys* 98:1372–1377
51. Lee C, Yang W, Parr RG (1988) Development of the Colle-Salvetti correlation energy formula into a functional of the electron density. *Phys Rev B* 37:785–789
52. Kim CH, Park J, Seo J, Park SJ, Joo TJ (2010) Excited state intramolecular proton transfer and charge transfer dynamics of a 2-(2'-hydroxyphenyl)benzoxazole derivative in solution. *Phys Chem A* 114:5618–5629
53. Santra M, Moon H, Park MH, Lee TW, Kim Y, Ahn KH (2012) Dramatic substituent effects on the photoluminescence of boron complexes of 2-(benzothiazol-2-yl)phenols. *Chem Eur J*. doi:10.1002/chem.201200726
54. Li H, Niu L, Xu X, Zhang S, Gao F (2011) Excited state proton transfer in guanine in the gas phase and in water. *J Fluoresc* 21:1721–1728
55. Furche F, Rappaport D (2005) Density functional theory for excited states: equilibrium structure and electronic spectra. In: Olivucci M (ed) *Computational photochemistry*, vol 16, Chapter 3. Elsevier, Amsterdam
56. Lakowicz JR (1999) *Principles of fluorescence spectroscopy*, 2nd edn. Kluwer Academic, New York
57. Valeur B (2001) *Molecular fluorescence: principles and applications*. Wiley-VCH Verlag, Weinheim
58. Frisch MJ, Trucks GW, Schlegel HB, Scuseria GE, Robb MA, Cheeseman JR, Scalmani G, Barone V, Mennucci B, Petersson GA, Nakatsuji H, Caricato M, Li X, Hratchian HP, Izmaylov AF, Bloino J, Zheng G, Sonnenberg JL, Hada M, Ehara M, Toyota K, Fukuda R, Hasegawa J, Ishida M, Nakajima T, Honda Y, Kitao O, Nakai H, Vreven T, Montgomery JA Jr, Peralta JE, Ogliaro F, Bearpark M, Heyd JJ, Brothers E, Kudin KN, Staroverov VN, Kobayashi R, Normand J, Raghavachari K, Rendell A, Burant JC, Iyengar SS, Tomasi J, Cossi M, Rega N, Millam NJ, Klene M, Knox JE, Cross JB, Bakken V, Adamo C, Jaramillo J, Gomperts R, Stratmann RE, Yazyev O, Austin AJ, Cammi R, Pomelli C, Ochterski JW, Martin RL, Morokuma K, Zakrzewski VG, Voth GA, Salvador P, Dannenberg JJ, Dapprich S, Daniels AD, Farkas O, Foresman JB, Ortiz JV, Cioslowski J, Fox DJ (2010) *Gaussian 09*, revision C.01. Gaussian, Inc, Wallingford
59. Padalkar VS, Patil VS, Sekar N (2011) Synthesis and characterization of novel 2, 2'- bipyrimidine fluorescent derivative for protein binding. *Chem Central J* 5(72):1–7
60. Padalkar VS, Patil VS, Sekar N (2011) Synthesis and photophysical properties of fluorescent 1,3,5-triazine styryl derivatives. *Chem Central J* 5(77):1–9
61. Patil VS, Padalkar VS, Phatangare KR, Gupta VD, Umape PG, Sekar N (2012) Synthesis of new ESIPT-fluorescein: photophysics of pH sensitivity and fluorescence. *J Phys Chem A* 116(1):536–545
62. Padalkar VS, Ponnadurai R, Sekar N (2013) A combined experimental and DFT-TDDFT study of the excited-state intramolecular proton transfer (ESIPT) of 2-(2'-hydroxyphenyl) imidazole derivatives. *J Fluoresc*. doi:10.1007/s10895-013-1201-2
63. Padalkar VS, Patil VS, Telore RD, Sekar N (2012) Synthesis of novel fluorescent 1,3,5-trisubstituted triazine derivatives and photophysical property evaluation of fluorophores and its BSA conjugates. *Heterocyclic Commun* 18(3):127–134